ZIBELINE INTERNATIONAL™ PUBLISHING

Water Conservation and Management (WCM)

DOI: http://doi.org/10.26480/wcm.01.2026.116.126

ISSN: 2523-5664 (Print)
ISSN: 2523-5672 (Online)
CODEN: WCMABD

RESEARCH ARTICLE

ANALYSIS OF CLIMATE CHANGE IMPACT ON SPATIAL AND TEMPORAL PRECIPITATION PATTERNS IN IRAQ THROUGH ANALYSING CRU GRIDDED DATASETS USING REMOTE SENSING TECHNOLOGY

Noor N. Yasir* and Hayder H. Kareem

Structures and Water Resources Engineering Department, Faculty of Engineering, University of Kufa, Al-Najaf, Iraq
**Corresponding Author Email: noorn.alfahham@student.uokufa.edu.iq*

Article History:

Received 27 January 2026
Revised 14 February 2026
Accepted 20 February 2026
Available online 11 March 2026

ABSTRACT

Climate change greatly influences ecosystems, communities, and economies. The effects of climate change on water supplies, environmental conditions, and weather patterns will typically have both abrupt and gradual impacts on all three categories. In Iraq, the geographical analysis focused on the annual concentration of precipitation. The high-resolution climate grid (0.5×0.5) used in this analysis provided information for the period of 1956 to 2025. It used an initial 5-year period and the final 5-year period within each decade. The use of Geographic Information Systems (GIS) enabled the study to achieve the objectives of this analysis. Rainfall figures reflect great variability among the rainfalls recorded within the different decades of the second millennium. In the 6th decade of the 20th century, annual rainfall ranged from 21–1047 mm, in the seventh decade between 32–1080 mm, in the 8th decade between 105–1082 mm, in the 9th decade between 110–1037 mm, and in the 10th decade between 98 – 1091 mm. Even though there were large fluctuations from one rainy season to another, both 5-year periods within each of the three decades had relatively consistent rainfall amounts, while there was a pronounced decrease from monthly to long-term intensity during the first and second decades of the third millennium. The total volume of precipitation recorded was significantly lower than the previous two decades; for example, during the first decade of the 3rd millennium total amount of precipitation was 114–986 mm, and during the second decade total amount of precipitation was 89–987 mm. Precipitation has been highest near those regions which experience the most rainfall (northeast and north), while precipitation amounts are substantially less in southern and southwest Iraq. The annual rainfall averages are well below those seen at the end of the twentieth century and over the last few decades as a consequence of climate change. The average annual precipitation amounts from the rainfall maps vary from 76 mm to 1,014 mm, while the average annual precipitation amount for the 2010's was 1,065 mm. The northern areas have consistently received more precipitation than the southern areas, which are mostly dry. Therefore, Iraq is already suffering from decreased precipitation due to the ongoing effects of variability in rainfall patterns. As a result, there is an urgent need to examine different sources of water and the efficient use of what falls as precipitation.

KEYWORDS

Spatial Analysis; Climate Change; Precipitation Rates; CRU; GIS; Iraq.

1. INTRODUCTION

Precipitation intensity is the most important characteristic used to define a place's or region's climate, as it complements the most commonly used conventional determinants of climate – annual precipitation totals and seasonality. Intensity of precipitation is important in helping to assess the hazard potential associated with extreme precipitation events (Seneviratne and Neville, 2012; Donat et al., 2013). Therefore, in order to be able to successfully evaluate and delineate precipitation patterns at the regional scale, high temporal and high spatial resolution data are needed. The reason for such precision is that precipitation varies greatly over time and space, thereby requiring that data be collected and presented in a very high-resolution format. Multiple researchers have identified the growing importance of high-quality, gridded data sets within climate science research, (Trenberth, 1997; Goddard et al., 2001). Naturally, high-quality, gridded data sets that have been subject to exhaustive quality control measures and include long-term historical climate records are of great importance. In recent years, there has been an increased demand for the availability of high-resolution, temporally and spatially representative gridded data sets that are comprehensive and continuously updated. Such data sets have wide-ranging applicability across many areas, including hydrology, agriculture, and human health. As demonstrated the necessity of utilizing gridded data in evaluating and verifying global and regional climate models (Osborn and Hulme, 1997). In addition, statistical downscaling methods, as described, are critical for producing specific regional climate forecasts that can effectively use global-scale forecasts by (Maurer and Hidalgo, 2008). However, the ongoing anthropogenic release of greenhouse gases into the atmosphere continues to cause dramatic changes in precipitation patterns due to climate change. Numerous studies have examined the complex relationship between climate change and

Quick Response Code	Access this article online	
	Website: www.watconman.org	DOI: 10.26480/wcm.01.2026.116.126

Cite The Article: Noor N. Yasir and Hayder H. Kareem (2026). Analysis Of Climate Change Impact on Spatial and Temporal Precipitation Patterns in Iraq Through Analysing Cru Gridded Datasets Using Remote Sensing Technology. Water Conservation and Management, 10(1): 116-126.

shifting precipitation patterns. The prominent world organization (IPCC) has published specific assessment reports highlighting projected rainfall scenarios and current observations about changes in the amount of precipitation occurring. In addition to this, both the IPCC 5th Assessment Report (2014) and the 6th Assessment Report (2021) provide large amounts of information regarding trends in precipitation, along with a greater understanding of the hydrological cycle and dynamic atmospheric change. Increasing global temperatures, as a result of climate change caused through warming of the Earth, increase the rate at which the oceans and rivers evaporate, causing greater amounts of humidity to be in the atmosphere. This could cause increased numbers and intensity of rain events in some areas, while other areas will show decreases in precipitation. As a result of climate change, many parts of the world are now experiencing increased severity of heavy rain and flood events. On the other hand, some areas may receive less precipitation because of changes to the atmospheric circulation patterns associated with climate change (Cai et al., 2014). Results from these changes will vary between different regions as local factors interact with up-to-date global climate conditions. An example of this includes the recent rapid increase in temperatures in the Arctic and other northern latitudes, creating a transition from snow to rainfall-type precipitation, resulting in changing ecosystems within the Arctic and creating additional challenges for indigenous peoples (Groisman et al., 2005). The volume of research focused on analyzing the spatial and temporal distribution of rainfall events represents a critical area of study that is creating important information regarding the complex processes associated with climate variability, especially as climate variability relates to adaptation to climate change. With advances in environmental modelling, scientists are able to analyse and predict the future distribution of rainfall events across multiple climate change scenarios (Trenberth et al., 2003). Datasets with much greater geographic and temporal resolutions are needed for regional and local evaluations, where spatial scales of tens of kilometers and intra-daily or daily temporal resolution are commonly used to evaluate atmospheric variability between sub-regions and to carry out a comprehensive assessment of both normal and abnormal climate. In recent years, there have been considerable advancements toward the development of daily gridded datasets of global extent, created through the integration of vast networks of daily precipitation observations from many different observational networks. Additionally, gridded datasets for many non-global regions have also been developed, achieving spatial resolutions of around 50 km, resulting in sufficient data to support the evaluation of many global environmental issues across large areas of inland regions. Including for Europe, for North America, for South America, and for Asia, each of these studies highlights the gridded datasets developed for their respective regions (Haylock et al., 2008; Maurer and Hidalgo, 2008; Liebmann and Allured, 2005; Yatagai et al., 2009). As used high-resolution satellite data to examine the spatial distribution of rainfall over India, attempting to identify local patterns and trends in precipitation over the last decade and a half (Mishra et al., 2022). Similarly, utilized satellite-based data and advancements in remote sensing technology to conduct a global analysis of rainfall, examining the spatial and temporal variability of precipitation across the globe (Behrangi et al., 2021). To understand patterns of rainfall, environmental models are critical. As developed models replicating meteorological conditions to examine precipitation across South Asia to identify significant temporal and spatial trends (Shekhar et al., 2020). The Global Precipitation Measurement (GPM) project, as described, is a national endeavour that delivers continuous and highly accurate rainfall data for global climate studies, utilizing satellite technology (Huffman et al., 2017). As performed a longitudinal study in China investigating extreme fluctuations in precipitation through scale analysis and satellite data (Zhang et al., 2019). Examined local and temporal patterns of rainfall variability in the Himalayan region (Swain and colleagues, 2022). As conducted a thorough global evaluation of long-term alterations in precipitation, focusing specifically on the effects of anthropogenic environmental change (Zhang et al., 2021). Furthermore, investigated the impact of urbanization on spatial rainfall distributions in metropolitan environments (Song et al., 2021; Donat et al., 2013). To proficiently assess and delineate the regional-scale. To analyze precipitation patterns, it is crucial to utilize data with elevated temporal and spatial precision. This degree of accuracy is essential because of the swift fluctuations in precipitation across time and geography. The value of high-quality, gridded datasets has been underscored by numerous researchers, notably, who stressed their increasing relevance in climate research (Trenberth, 1997; Goddard et al., 2001). Gridded datasets, subjected to rigorous quality control, and meteorological spatial data that correspond with observational data are crucial across various scientific disciplines, including environmental science, hydrology, agriculture, renewable energy, biology, economics, and sociology (Sun et al. 2018). Precipitation is a crucial determinant of the hydrological cycle and is frequently the most difficult quantity to quantify. Precipitation records are essential for informing hydrological models, including the Soil and Water Assessment Tool (SWAT), Geographic Information System (GIS), and the Topography-Based Hydrological Model (TOPMODEL), as well as for environmental validation (Fick and Hijmans, 2017).

Interpolation methods utilize data from localized weather networks, atmospheric reanalysis products, weather radar, satellite data, or a combination of these sources to create global or local gridded rainfall datasets. Each of these methods possesses flaws, several of which are especially evident in precipitation estimation. Although the spatial and temporal resolution of weather radar is excellent, the range is typically limited (Beck et al. 2017a). In particular, locations with complex terrain can be difficult to assess because many of the data sources that will be used to create precipitation grids (e.g., satellite information, reanalysis, modelled adaptation, and statistical downscaling) often have difficulties accurately providing data, due in part to the high spatial, temporal, and geographical variability of such areas (Beck et al. 2017a; Chen et al. 2014; Herold et al. 2016; Zambrano et al. 2017). Several researchers have identified the limitations of these datasets (Sun et al. 2018; Nastos et al. 2016; Beck et al. 2017b; Camera et al. 2017; Liu et al. 2017; Hu et al. 2018; Timmermans et al. 2019). As technological advancements take place and methodologies evolve, synergies between machine learning and crowd-sourced information may be essential to enhancing the quality of and usability of many data sets for climate-related applications (Sun et al. 2018). Several recent studies have focused on using spatial modelling and gridded climate data to investigate the impacts of global climate change on sources of freshwater. For example, investigated trends in rainfall in the state of Arizona, USA, from 1961 to 2022, using high-resolution gridded datasets available through the CRU (Kareem et al., 2024a, Kareem et al., 2024b, Kareem et al., 2025). Their analysis, using GIS methods, identified fluctuations in earlier years; however, there was a significant downward trend in the occurrence of rainfall in the early 2000s, which they attribute to increasing climate change. Similarly, investigated the impacts of rainfall change scenarios in Iraq using PRECIS regional climate models for the historical period of 1951-2020 and projected rainfall scenarios for the years leading up to the year 2050(Al-Azawi et al. 2024). This research utilized two spatial interpolation techniques, Inverse Distances Weighting (IDW) and Kriging, to develop and evaluate prediction maps of rainfall amounts in Iraq. The results of the research indicated that the IDW technique provided the most accurate forecasts. The research documented the projected averages of total annual rainfall to decrease annually until 2050 and illustrated the need for improved methods of managing water resources. (Najah Sarmad et al. 2025). The research utilized Remote Sensing (RS) and Geographic Information Systems (GIS) technologies to estimate and validate the amount of rainfall in Iraq during 2011-2020 by reviewing and digitally processing a total of (120) high-resolution satellite images using Kriging interpolation. The results of the analysis showed evidence of wide spatial variation in the amount of precipitation. The northwest areas experienced the highest rates of precipitation, and the western and southern areas had the lowest rates of precipitation, with a maximum recorded amount of 729.22 mm. The research concluded that satellite images and GIS technologies are efficient and dependable methods of predicting rainfall patterns, especially in areas without ground observation stations. In their analysis, studied the monthly rainfall trend at 39 separate meteorological stations over the period from 1980 to 2021 (Sara.A.Muter et al., 2025). The research indicated that rainfall patterns in Iraq are highly dynamic and irregular, and that there is evidence of a general decline in rainfall across most meteorological stations, with the exception of the stations located in Baghdad, Kut, Hilla, Amarah, and Samawah. The results indicated that as you move from the northern region (Duncan Station) towards the southern and western regions (Nukaib Station), precipitation declines significantly in each region. The 42-year study found that in 2021, Iraq experienced its lowest recorded levels of precipitation and the driest year in the last 42 years. Although northern regions typically receive the largest amounts of rainfall, there is also a higher level of standard deviation, which means rainfall levels are more variable or erratic. In an effort to describe what weather systems are influencing Iraqi weather and climate. (Aljuhaishi et al.2025) evaluated spatiotemporal variations of pressure systems in Iraq from 1999 to 2020. Findings indicate that five primary weather systems travel across Iraq: the Monsoon low, the Siberian high, the Red Sea depression, the Subtropical high, and the Mid-Latitude depression. Findings also concluded that the Monsoon low is the dominant weather system and prevails for approximately 126 days each year, and is especially prominent in the southern region during summer months, while the Siberian high predominates during winter, about 70 days a year, and is most noticeable in the northern region of Iraq. The Red Sea Depression is the most predominant in the spring and occurs on average 60 days each year, while the Mid-Latitude Depression is rarely seen, occurring approximately 7 times per year, chiefly in the central region. Because of the complex interaction of different weather-related elements, as well as

human influences such as population growth, the effects of climate change on precipitation patterns are a very complicated set of problems. Analysis of temporal and spatial patterns of precipitation in Iraq is an important area of study that has provided valuable insights into the many different processes behind climate variability and change. The precipitation patterns in Iraq will be analyzed in five-year intervals since 1956 to assess the influence of Earth's climate system on this region and to investigate notable temporal and spatial variations utilizing high-resolution satellite images. Furthermore, precipitation trends for each decade will be analyzed to evaluate the impacts of climate change from 1956 to 2025.

1.1 Study area

Iraq is located in the southwestern part of Asia and the northeastern area of the Arab world. Its astronomical position, delineated by latitude and longitude, is situated between the latitudinal coordinates of 29° - 37° north and the longitudinal coordinates of 38° - 48° east, yielding an east-west extension almost equivalent to its north-south length. The terrain of Iraq comprises a vast continental basin extending from the Turkish highlands in the northwest to the Arabian Gulf in the southeast, bordered by a desert, referred to as the western plateau, to the west and mountain ranges to the east. Iraq is bordered to the north by Turkey, to the east by Iran, and to the west by Syria, Jordan, Saudi Arabia, and Kuwait to the south (The Geography of Iraq, Al-Dabbas et al.).

The climate is predominantly continental, subtropical, and semi-arid. The mountainous region exhibits a Mediterranean climate. Rainfall typically transpires from December to February or from November to April in the mountainous terrain. In winter, the average daily temperature is approximately 16°C, decreasing to 2°C at night with a potential for frost. During the summer, temperatures exceed 45 °C on average in July and August, decreasing to 25 °C at night (Al-Ansari, 1988, 2013; Al-Ansari et al., 1981; Al-Ansari and Knutsson, 2011). Table 1 represents the weather systems throughout Iraq over time periods involving specific large-scale atmospheric systems affecting geographical areas at specified times of the year. The most important atmospheric system is the Monsoon Low, which has a major effect on Southern Iraq for approximately 126 days of the year; it primarily occurs during the summer months. The second major atmospheric system is the Siberian High that typically exists in winter and affects Northern Iraq for around 70 days; after this time period, it gradually dissipates from the region. The third major atmospheric system is the Red Sea Depression, which will occur in transition into spring for approximately 60 days. The Fourth atmospheric system, the Mid-Latitude Depression, is much rarer, having been known to occur an average of about seven times annually, with most activity occurring in Central Iraq. Iraq displays considerable diversity in its topography, consisting of four main regions. The mountainous area in northern and northeastern Iraq constitutes 5% of the nation's total land area. The elevation in this region ranges from 1000 to 3600 meters above sea level. The semi-mountainous region, situated south of the initial area, comprises 15% of Iraq's total landmass, with altitudes varying from 200 to 1000 meters above sea level. The alluvial plain region is located between and next to the lower parts of the Tigris and Euphrates rivers. It runs from central to southern Iraq and makes up 20% of the country's total land area. The western desert region comprises 59.5% of Iraq's total area, with altitudes varying from 100 to 1000 m above sea level. Topographical variables in Iraq can directly affect and generate significant local climate differences between the northern and southern portions of the country. In contrast, approximately two-thirds of the country is lowland, positioned at an elevation of 200 meters or lower above sea level. Table 2 represents the landscape of Iraq, which has an interesting variety of physical features because it can be divided into four separate regions that differ greatly in size and elevation. The largest region, the Western Desert Plateau, covers about 29% of Iraq's land area and is classified as having an extremely dry climate with the least amount of precipitation. In contrast, the Mountainous Region is comparatively quite small (about 5% of Iraq's total land area) and is also the area with the greatest amount of hydrological activity in the country, having the highest elevation (up to about 3600 m.a.s.l.) and receiving the greatest amount of rainfall and snowfall. The Sedimentary Plain occupies approximately twenty percent of Iraq's territory at the lowest elevations (at about 200 m.a.s.l. or less) and follows the course of the Tigris and Euphrates rivers near their respective mouths. The Semi-Mountainous Regions, at approximately 15% of Iraq's total land area, are a transitional region to the south of the mountains and are at elevations between 200 and 1000 m.a.s.l. Thus, there are no significant regional variations in the orographic climate within these regions (Al-Ansari 2021). Iraq is experiencing increased desertification, more frequent dust storms, and overall hotter weather. The crux of the matter is the progressive irregularity, in consistency and frequency, and distribution of the precipitation.

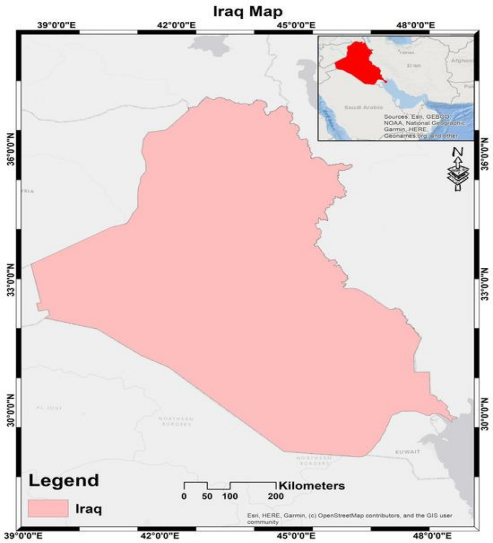

Figure 1: Republic of Iraq

Table 1: Main weather systems and their temporal and spatial influence in Iraq

Atmospheric Systems	Annual Dominance (Days/Year)	Dominant Season	Main Geographical Influence
Monsoon Low	~ 126 Days	Summer	Dominant system, most prominent in the Southern region
Siberian High	~ 70 Days	Winter	Most prominent in the Northern region
Red Sea Depression	~ 60 Days (Avg.)	Spring	Most prominent during Spring
Mid-Latitude Depressions	~ 7 Times per Year	Rarely noticed	Most prominent in the Central region

Table 2: Topographical and area characteristics of climatic regions in Iraq

Geographical Region	Total Area (%)	Height (m.a.s.l.)	Hydrological Characteristics
Mountainous Region (N and NE)	5%	1000 – 3600	Highest Rainfall rates
Semi Mountainous Region	15%	200 – 1000	Located immediately south of the Mountainous region
alluvial Plain (Central and South)	20%	≤ 200	located along the lower reaches of the Tigris and Euphrates rivers
Western Desert Plateau	59.5%	100 – 1000	Lowest Rainfall rates

1.2 CRU downloaded data

The Climatic Research Unit (CRU) has been used to obtain climate data for the research subject and has greatly assisted in the development of statistical software packages and climate models generally used. Also, CRU contributed to the construction of global temperature records used for monitoring climate system changes (Shi et al. 2017). Established in 1972 inside the university's School of Environmental Sciences, the inception of CRU was significantly shaped by the crucial contributions of prominent individuals. Included are Sir Graham Sutton, a former Director-General of the Meteorological Office; Lord Solly Zuckerman, an advisor to the University; and Professors Keith Clayton and Brian Funnel. Professors Clayton and Funnel served as deans of the School of Environmental Sciences in 1971 and 1972. Upon its establishment, CRU delineated four enduring objectives (Harris et al. 2020): 1) Augment the comprehension of historical climate patterns, encompassing both contemporary and ancient eras, 2) Implement worldwide surveillance and documentation of current climatic changes, 3) Look into the basic processes that cause climate change, whether they are natural or man-made, and figure out when they happen, and 4) Investigate the viability of disseminating advisory statements regarding forthcoming weather and climate trends, ranging from seasonal to multi-year projections, based on scientifically validated methodologies and articulated in a way conducive to long-term planning objectives.

CRU generates many climate datasets, encompassing global and regional metrics of temperature, precipitation, pressure, and atmospheric circulation. Among its most significant accomplishments is the CRUTEM global dataset, which monitors anomalies in near-surface land temperatures using a 5° by 5° grid format. The Hadley Centre for Climate Prediction and Research provides the sea-surface temperature dataset required to create the HadCRUT temperature record. As a result, these two organizations work in close collaboration to compile this dataset. This database, established in the 1980s, meticulously monitors worldwide temperature variations dating back to the 1850s. The bulk of the terrestrial section of this record has been compiled by the CRU; all of the marine section has been the product of the Hadley Center. The IPCC relies heavily on this assembled record as one of its primary sources for all of its many Reports and assessments. and in addition provides the CRU TS high-resolution gridded land surface dataset comprising various environmental variables. The CRU is mainly focused on the climate of Europe (the last 200 years or so), but incidentally to that activity has researched the climate of Eurasia. Climate for the last 10,000 years. A study of tree rings in the continent, and temperature records are used to examine the climate in Eurasia over the same period (Osborn and Jones, 2014). The CRU TS is a very often used climate dataset at a grid resolution of 0.5° latitude X 0.5° longitude, covering all non-Antarctic land on the Earth and produced by interpolating monthly climate anomalies computed using large networks of weather station observations .An initial version of CRU TS was released in 2000 and originally relied on the Angular Distance Weighting (ADW) method to interpolate observed anomalies from monthly observations to a 0.5° grid, covering global land areas. Six variables were originally provided; however, CRU TS has grown to ten variables since an update in 2004, which was followed in 2005 by further development—it has now been updated annually from 2006 to the present. It say that since its inception in 2000, the dataset has become established and widely used in a broad range of disciplines and applications (including local modelling impacted by weather and climate, such as river catchment modelling and agronomic studies, global and regional climate modelling, reanalysis bias correction, and paleoclimate reconstructions) (Osborn et al., 2019). Other than climate researchers, users of CRU TS also come from civil engineering, banking, etc. Meteorological observations are critical as input for estimating precipitation across large areas in Iraq; for example, many sites do not have ground observations. Thus, these databases are influenced by various spatial factors, integrating data from ground-based weather stations, satellites, and climate models. Suppliers of high-resolution rainfall data have made the downloaded datasets useful for analysing and computing the hydrological status of the area of concern, which helps to pinpoint environmental conditions in the area that may have changed as per the variability in the weather through the study period. Transactional data can be widely analysed at very high accuracy on a rain-spot basis through interpolation methods such as Kriging or Inverse Distance Weighting, which take into consideration the variations in the region where higher points of observation lie relative to other points, giving an overall picture of the render across some scales. This research will download rainfall data for Iraq from 1956 to 2025. This data will be evaluated annually to determine the magnitude of both adverse and beneficial climate changes in precipitation rates for these years.

The backbone analytical function of GIS is the overlay of spatially referenced data layers, which allows delineating their spatial relationships. However, it is also true that data used in GIS are predominantly static in nature, and most of them are collected on a single occasion and then archived. GIS today is far broader and harder to define. Many people prefer to define its domain as geographic information science and technology (GISandT), and it has become embedded in many academic and practical fields. The GISandT field is a loose coalescence of groups of users, managers, academics, and professionals all working with geospatial information. Each group has a distinct educational and "cultural" background. Each identifies itself with particular ways of approaching particular sets of problems. Over the course of development, many disciplines have contributed to GIS. Therefore, GIS has many close and far "relatives." Disciplines that traditionally have researched geographic information technologies include cartography, remote sensing, geodesy, surveying, photogrammetry, etc. Disciplines that traditionally have researched digital technology and information include computer science in general and databases, computational geometry, image processing, pattern recognition, and information science in particular. Disciplines that traditionally have studied the nature of human understanding and its interactions with machines include cognitive psychology, environmental psychology, cognitive science, and artificial intelligence. In developing a core curriculum for GIS, the University Consortium for Geographic Information Science suggests that "GISandT should not be defined by merely linking segments of the traditional domains (e.g., cartography, remote sensing, statistical analysis, locational analysis, etc.), but rather by placing the emphasis directly upon concepts and methods for geographic problem solving in a computational environment (UCGIS, 2003)." GIS should not be viewed merely as a col lection of tools and techniques. Rather, the scope of GISandT represents "a body of knowledge that focuses in an analytic fashion upon various aspects of spatial and spatiotemporal information and therefore constitutes, in some of its aspects, a science" (UCGIS, 2003). GIS has been called or defined as an enabling technology because of the breadth of uses in the following disciplines as a tool. Disciplines that traditionally have studied the earth, particularly its surface and near surface in either physical or human aspects, include geology, geophysics, oceanography, agriculture, ecology, biogeography, environmental science, geography, global science, sociology, political science, epidemiology, anthropology, demography, and many more (Weng, 2010)

2. METHODOLOGY

2.1 GIS Processing of Climate Research Unit Data

To calculate the annual fall rates, it is essential to analyze the huge and intricate datasets obtained for the study area, which encompasses a protracted time frame and a significant part of Iraq. The subsequent operations will be executed with the aid of GIS software.

2.2 Create NetCDF raster layer

NetCDF (Network Common Data Form) consists of a collection of software libraries and data formats that are self-describing and interoperable across diverse computing environments. These tools assist in the creation, retrieval, and distribution of scientific data that is arrayed. NetCDF is highly suitable for storing data of many dimensions, including temporal and spatial data. It stores data and metadata together in a single file,

making access clearer to the consumer. This file formatting is also useful in situations where access to vast amounts of data is needed. The data acquired will be converted into NetCDF raster format in GIS programs. (Morice et al., 2021).

2.3 Data Projection

Spatial data, whether portrayed as points, lines, polygons, rasters, or annotations, is always created within a coordinate system. Coordinates can be described in many types of units, such as feet, meters, kilometers, or even decimal degrees. The first step in deciding on the correct coordinate system is working out the measuring system it sits underneath. The resultant coordinate system with the data is then projected onto a flat surface, such as a page of paper or your computer screen. This is worked by converting the coordinate system used on the curved surface of the Earth to flat surface equivalents by complex mathematics. The study will use the WGS 1984 UTM Zone 38N system to cover the whole of Iraq.

2.4 Composite Bands

The Climatic Research Unit (CRU) provides monthly rainfall data for Iraq, with the downloaded information categorized by decade. For the decade spanning 1960 to 1969, there are 120 monthly rainfall rates, corresponding to 120 raster pictures. Images were downloaded, with an equivalent quantity for the future decades (1956–2025). This project will investigate precipitation data in five-year. This indicates that 60 raster images will be amalgamated for each five-year interval. Raster datasets may comprise a singular band, denoting one attribute, or numerous bands. A band can be seen as a matrix of cell values, and in a multi-band raster, multiple matrices of cell values pertain to the same geographical region. Each cell in these bands contains multiple values, representing various segments of the electromagnetic spectrum observed by sensors. The electromagnetic spectrum encompasses the visible range as well as the infrared and ultraviolet ranges, frequently utilized in satellite imagery. During the creation of map layers from raster pictures, distinct data bands can be amalgamated into a composite band, exemplified by the RGB (Red, Green, and Blue) color scheme. This technique allows many of the bands to be displayed at once, which promotes quick interpretation and retrieval of important data from the dataset. Looking at RGB composites gives more clues than one band work, as it uses many parts of the spectrum for a more complete analysis of rainfall. (Esri, ArcGIS Desktop Documentation, 2023).

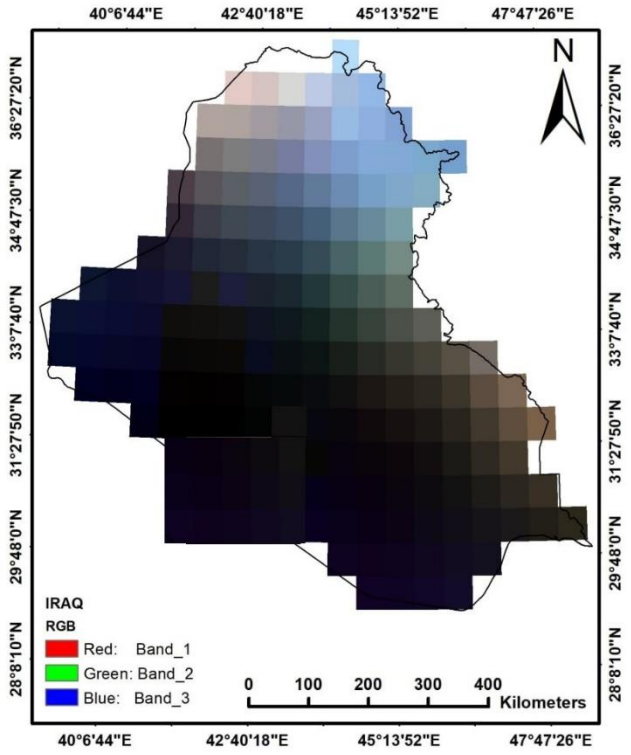

Figure 2: Extracted CRU Data as NetCDF raster format

2.5 Cell Statistics and Map Algebra

This geographical analysis function calculates a statistic for each cell in an output raster, using the values from cells in multiple input rasters. For statistical types such as Maximum, Minimum, Mean, Median, Majority, Minority, Percentile, and Sum, if a single raster is to be used as an input (as in this study, where a composite band is used for each decade, a cell in the output raster layer will have the same value as the only input raster. Map Algebra is a general-purpose, robust algebra used to execute all Spatial Analyst tools, operators, and functions for geographical analysis. Serving as a mathematical logic for the manipulation of spatial data predominantly in the form of fields, Map Algebra allows for the construction of a new raster layer from one or more raster layers of the same size, having cells that are to be manipulated using a mathematical or another user-specified operation (Jensen, 2016). For this research, composite bands are used on monthly rainfall data for five-year intervals in countries, and the statistics of cells are summed to ascertain the intensity of total rainfall for each interval. The yearly average rainfall intensity for each five-year interval will be calculated by dividing the aggregated value (resulting raster image) acquired from the cell statistics application by 5.

2.6 Conversion from Raster to Point

In this phase, the raster dataset showing the average annual precipitation over five-year intervals, produced during the Map Algebra process, will be converted into point features. For each cell in the raster dataset, a corresponding point will be created in the output feature class, representing the cell's center. The conversion will omit cells containing no-data values, ensuring that only cells with valid data are converted into points.

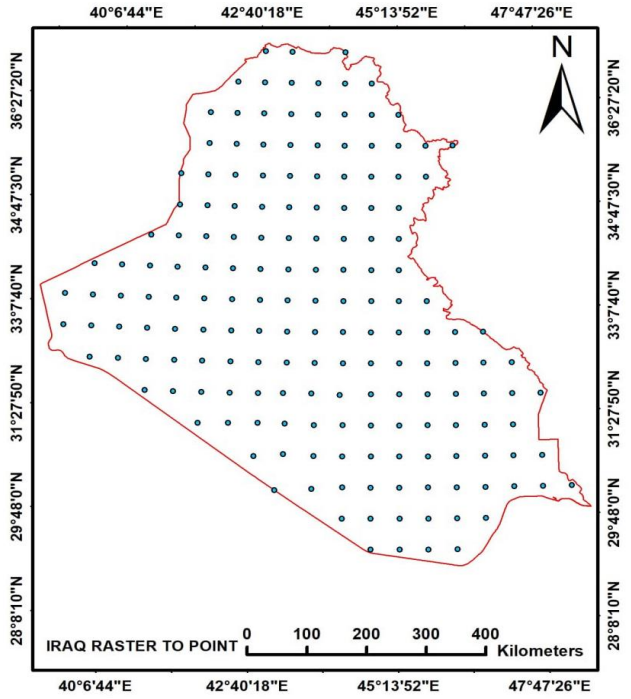

Figure 3: Raster to point

2.7 Interpolation Methodology (IDW Technique)

In recent years, GIS capabilities for spatial interpolation have improved by integration of advanced methods within GIS, as well as by linking GIS to systems designed for modelling, analysis, and visualization of continuous fields. Because it is impossible to cover all or even most of the existing interpolation techniques, only methods that are often used in connection with GIS or have the potential to be widely used for GIS applications are included, and references are given to the literature for more detailed descriptions.

All interpolation methods have been developed based on the theory that points closer to each other have more correlations and similarities than those farther apart. In the IDW method, it is assumed substantially that the rate of correlations and similarities between neighbors is proportional to the distance between them, which can be defined as a distance reverse function of every point from neighboring points. It is necessary to remember that the definition of the neighboring radius and the related power to the distance reverse function are considered important problems in this method. This method will be used by a state in which there are enough sample points (at least 14 points) with a suitable dispersion in local scale levels. The main factor affecting the accuracy of the inverse distance interpolator is the value of the power parameter p (Burrough and McDonnell, 1998). In addition, the size of the neighborhood and the number of neighbors are also relevant to the accuracy of the results. (Setianto, A. et al. 2013). The advantage of IDW is that it is intuitive and efficient. This interpolation works best with evenly distributed points (M. Azpurua et al. 2010).

$$Z_p = \frac{\sum_{i=1}^{n} \frac{z_i}{d_i^p}}{\sum_{i=1}^{n} \frac{1}{d_i^p}}$$

Where:

Z_p: Estimated value at the unsampled location,

Z_i: Observed value at sampled point I,

d_i: Distance between the estimated point and point i, and

p: Power parameter (weighting power).n: Number of known points.

3. Result and Analysis

This section reviews the patterns of precipitation climatology in Iraq, where rainfall distribution is fundamentally shaped by the significant topographical variations between the northern and northeastern regions and the central and southern plains, with the physical geography of the Halgurd-Sakran (Hassarost) and Zagros mountain ranges playing a pivotal role in defining the country's rainfall map. Lifting of moist air from the Mediterranean owing to orographic forces results in heavy rains in the northern and northeast areas exceeding 1,000 mm on some peaks, while in the Western Plateau and lowland plain areas, they lie within a semi-arid region due to the gradual increase in height. Being within the subtropical zone, Iraq falls under a regime of winter rainfall of Mediterranean type, with rain confined to winter and spring, and all summer remains without rain, owing to the escape of clouds and rain owing to the prominence of the subtropical belt of high-pressure area. These patterns of rainfall vary in accordance with climatic regions, from that of the Mediterranean mountain climate with its considerable rain and snow, through the steppe zone to the deserts of Iraq proper where very slight and sporadic rain is followed, when necessary, by direct dependence on the discharge of the Tigris and Euphrates; the degree and duration of the fall being affected by the incursions of frontal depressions from the Mediterranean (the body of air rising thereafter) which may on occasion combine with the Sudanese Thermal Low to lead to a dangerously unstable atmosphere and violent rainstorms in a short space of time, particularly over the central and southern parts of Iraq, thus producing a whole system of climatic extremes in the contrast between a rainy north and a dry south. Figure 4 gives the gradations of the annual rainfall in Iraq for (1956-1960) period Darkest green is the colour in the arid plains of the south where the minimum occurred (21.622 - 135.581 mm); the isohyet then steadily rises until the last tier of central light green and pale yellow is reached (up to 477.460 mm of rain), with the foothills of yellow and light brown isohyet of the north where the rain increases (477.460 - 705.379 mm). The extreme north highland areas, shown in white and rose-pink shading, receive maximum concentrations of (933.298 - 1,047.257 mm). As fivefold of that of the desert area of the south. In the next period (1961–1965), a very steep gradient of precipitation is again shown, the lowest observed in the south and southwest desert plateaux (32.160–148.619 mm). As we proceed to the intermediate bands broadly down the centre of the area (265.077–497.995 mm), and thence to the mid to high ranges of the north (614.454–847.371 mm), the rates mount towards the extreme north border where the strongest maxima (963.830–1,080.289 mm) occur. This shows clearly the vast difference in distribution of rain; the highlands have historically more than thirty times the annual precipitation of the southernmost. In the (1966–1970) interval sketch, the spatial distribution stresses the fact of a litter climatic feature, with precipitation mounting regularly from south to northeast. The arid southern deserts which moods effectually (dark green), exhibit the minimal (105.204–213.841 mm), increases in central areas of a quarter fold or more (322.479–539.754 mm) followed, until in the northern highlands (648.391–865.666 mm) ride the gradients in one of the most markedly rapidly increasing areas anyway, between pink and white (974.303–1,082.941 mm). All told, approaching ten times the delivery of the cruellest regions represented. Located between (1971–1975), the spatial scheme illustrated sets out that the gradient presses from south to north, with the dry desert (dark green) representing the lowest (111.644–214.555 mm), increasing through the middle light green and plain yellow belts (214.555–420.378 mm), and thence into the brown and pink mountainous north. The maximum is reached in the extreme north (934.934–1,037.845 mm), again squaring the off analogous contrasts not only of wet and the desolate swards. Looking at the (1976–1980) period, the dominance of the arid desert climate in the south restricts moisture to the lower, with the lowest rainfall (110.338–211.575 mm) within this dark green zone. As the humidity of the atmosphere increases northwards, so does the rain, increasing through the semi-arid central light green and pale-yellow bands rainfall (211.575–414.050 mm). The effect of elevation and orographic lift is so great that this trend has acquired momentum in the highlands, where values shoot up through the deep yellow and light orange first and fifth transitions to peak in the extreme northern sectors (920.235–1,021.473 mm), once again indicating the strong topographical control over the distribution of the country's rainfall. Looking at the (1981–1985)interval, the dark green ink blot (arid southern and southwestern sectors), indicates for the most part, low precipitation (98.544–199.892 mm) due to very little atmospheric moisture and desert conditions, proceeding towards the topography, where moisture increases gradually through light green and pale yellow tiers (up to 402.587 mm) of moisture as we come, comparatively, to the central plains. In the northern highlands, orchestrated by orographic lift, yellow, orange, and brown zones then lead to climax in the extreme north (pink and white) (807.977–1,010.672 mm), indicating the extent of the divide: the mountainous sectors receive over ten times the rainfall received in the southern deserts. Moving on to the (1986–1990) interval, we find the lowest rainfall registered by the dark green southern and southwestern plains, where arid desert conditions prevailed (112.980–221.649 mm). More moisture gradually reached the lower central and mid northern areas (in yellow and light orange); thence, in the high north, rainfall values were quickly elevated through increasing altitude and orographic lift to the extreme north in the pink and white zone. Here figures soared to (982.332–1,091.001 mm). The distribution here is the same as that confirmed above; the northern mountainous reaches received approximately 10 times the annual precipitation measured in the driest south. That said, through the (1991–1995) interval, there is a kind of hiatus in which the desert south (now dark green) registered the lowest rainfall taken together, low moisture availability being the culprit (112.100–218.726 mm). Then precipitation increased across the central light green and pale-yellow reaches (325.352–538.605 mm), peaking yet again where the growing northern highlands turned to mountains. Steep increases resulted from lifting and overcoming elevation. In the end, we find heavier rainfall passing through the browns and dark browns reaching the extreme north at the pink and white zone of (1,071.736 mm). As before, the distribution basis accepted is that the comparatively drier quarters in the south only received about 9 times less rainfall than the northern mountains.

During the (1996-2000) period, southern and southwestern desert areas (dark green) exhibited very low mean annual rainfall (65,110-172,265 mm) attributable to extremely arid climatic conditions. Mean monthly relative humidity increased throughout the central and lower northern tier (light green and yellow zones), reaching (172,265-493,729 mm), as atmospheric moisture content increased; however, in the northeastern highlands, precipitation increased dramatically due to orographic lift from topography, peaking at 922.348-1,029.503 mm in the (light pink and white) areas. This distribution reflects that for this period, northern mountain regions received more than 15 times the annual precipitation amount of the arid deserts in the south. In the (2001-2005) period, the arid southern and southwestern (dark green) regions continued to receive the lowest average precipitation amount (114,254-211,139 mm) because of dry air and desert conditions. Average rainfall amounts increased throughout the central (light green and yellow) areas (211,139-501.796 mm), before sharply increasing in the northern foothills and mountains. In both the extremely northern (pink and white) regions, total amounts peaked between 792.452 mm and 986.222 mm as a result of increasing elevation and orographic lift. Comparatively, the northern mountainous region received 8 to 9 times as much annual precipitation as the southern arid regions. The (2006-2010) time period demonstrated similar climatic trends as prior time periods, where the arid southern desert (dark green) received the least average annual precipitation (117.984-211,552 mm); once again, this is because of limited moisture. Average precipitation amounts in the central (light green and yellow) gradually increased (305,121-492,257 mm), then sharply increased in the northeastern highlands, again as a result of increasing elevation and widespread orographic lifting processes. Due to topographic elevation and orographic lift, of the total annual rainfall received in precipitation peaked at (772.962–960.098 mm) at the extreme northern pink and white zones. This distribution demonstrates that the mountains of the northern part of the region historically received approximately eight times as much rainfall annually as the most arid southern sectors. In contrast, during the period of (2011–2015), the persistent climatic gradient remained as an arid desert in the southern part of the region (displayed in dark green) received the least amount of precipitation (89.232–188.992 mm) based on a lack of moisture. The amount of precipitation from the central part of the region increased (288.752–488.272 mm) and then increased very dramatically from the northern part of the region due to the topographic elevation and orographic lift. The northern part of the region saw precipitation accrue through the brown and dark brown tier (588.032–787.552 mm) before reaching the extreme northern pink and white zones at (887.312–987.072 mm). This distribution demonstrates that the northern mountains are

receiving nearly eleven times as much rainfall annually as the driest southern sector. In the (2016–2020) timeframe, the arid southern part of the region (the dark green) received the least amount of precipitation (76.140–180.413 mm) due to the continued low moisture availability. The amount of precipitation from the central part of the region increased (180.413–493.232 mm) and then increased dramatically from the northern part of the region Driven by topographic elevation and orographic lift, moisture levels intensified through orange and brown tiers, peaking in the extreme northern pink and white zones at (910.324–1,014.597 mm) . This contrast highlights that the northern highlands received over thirteen times the annual rainfall of the driest southern desert sectors. Finally, for the (2021–2025)period, the annual rainfall distribution confirms a persistent gradient, where the arid southern sectors dark green recorded the lowest totals (82.725–191.891 mm). Moisture levels increased across the central yellow and light orange bands (301.058–628.554 mm) before intensifying significantly in the northern foothills. Driven by rising topography and orographic lift, precipitation peaked in the extreme northern pink and white zones at 956.052–1,065.217 mm, indicating that the highlands received over twelve times the rainfall of the arid southern desert.

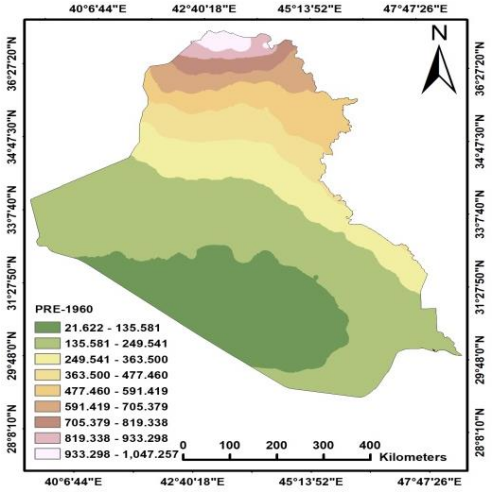

1960

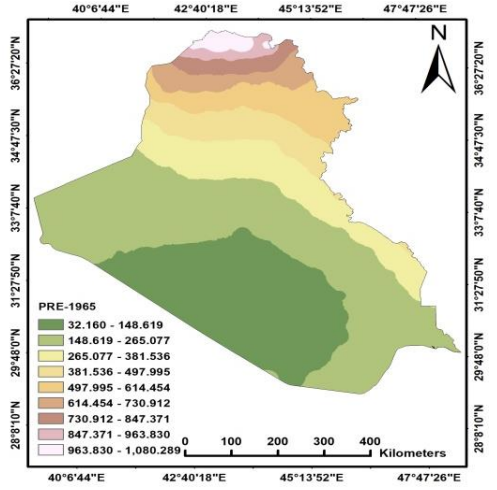

1965

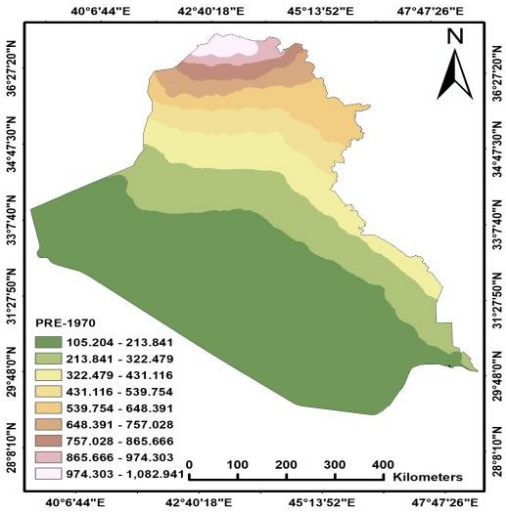

1970

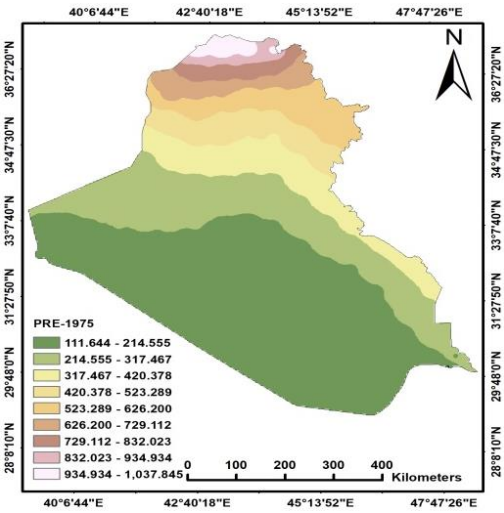

1975

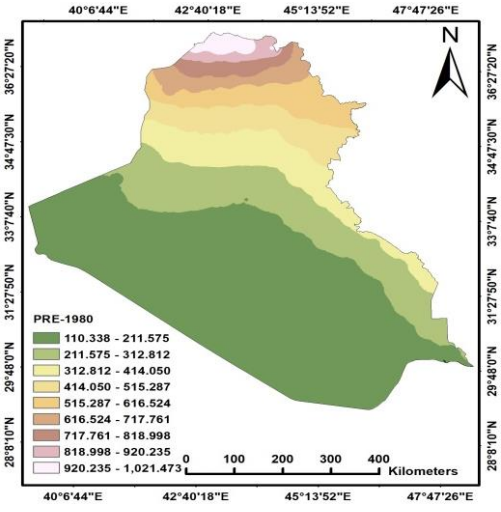

1980

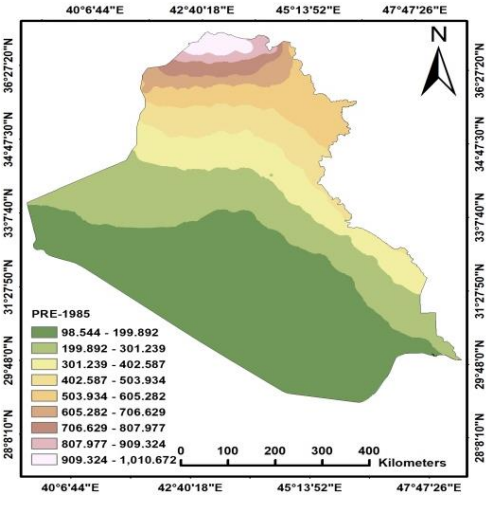

1985

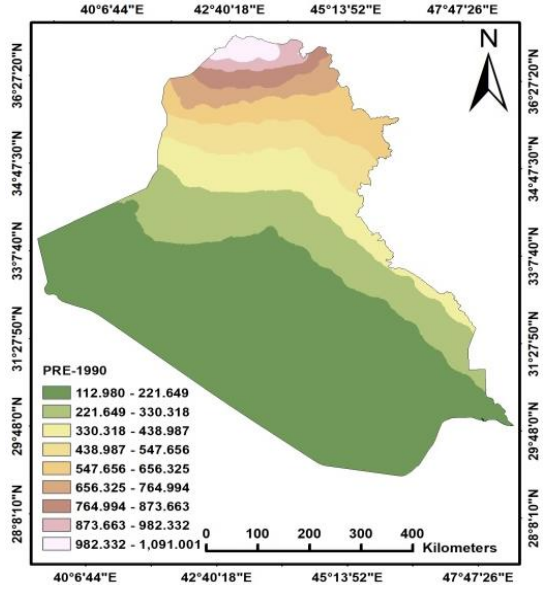

1990

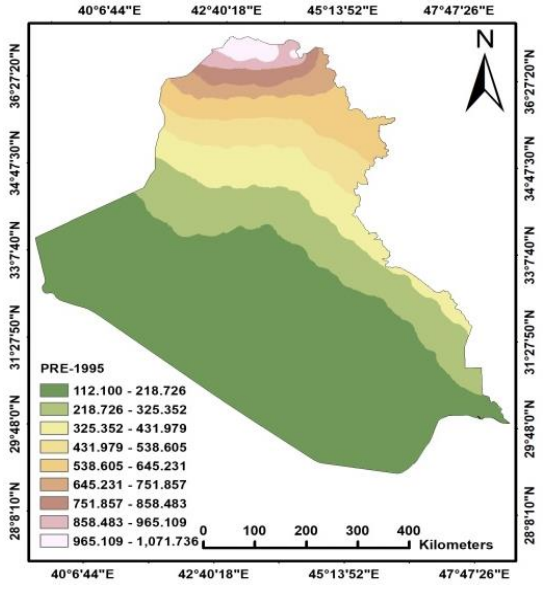

1995

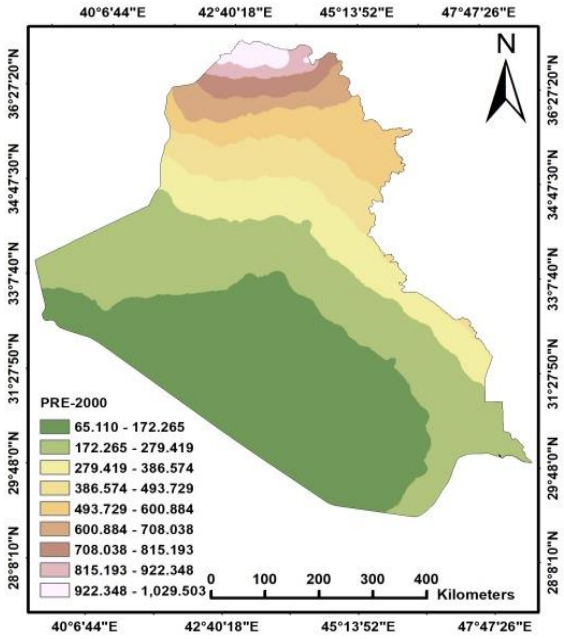

2000

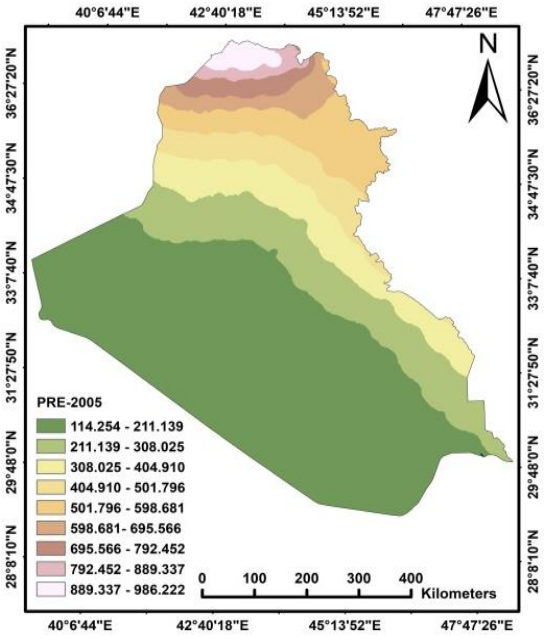

2005

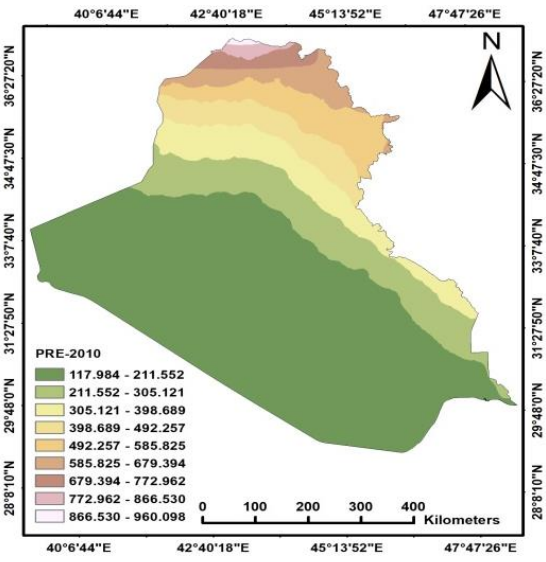

2010

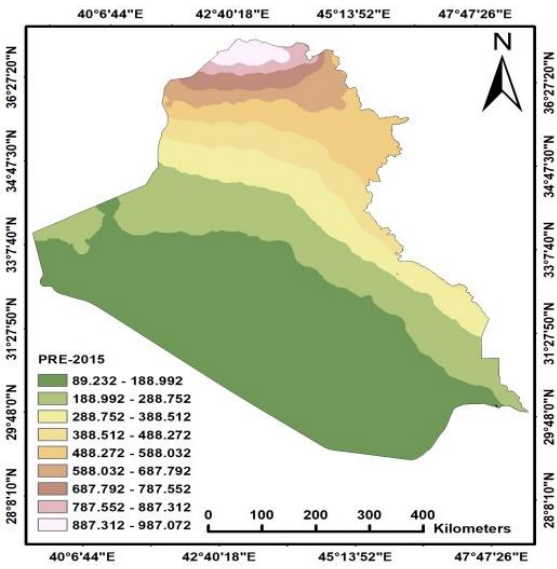

2015

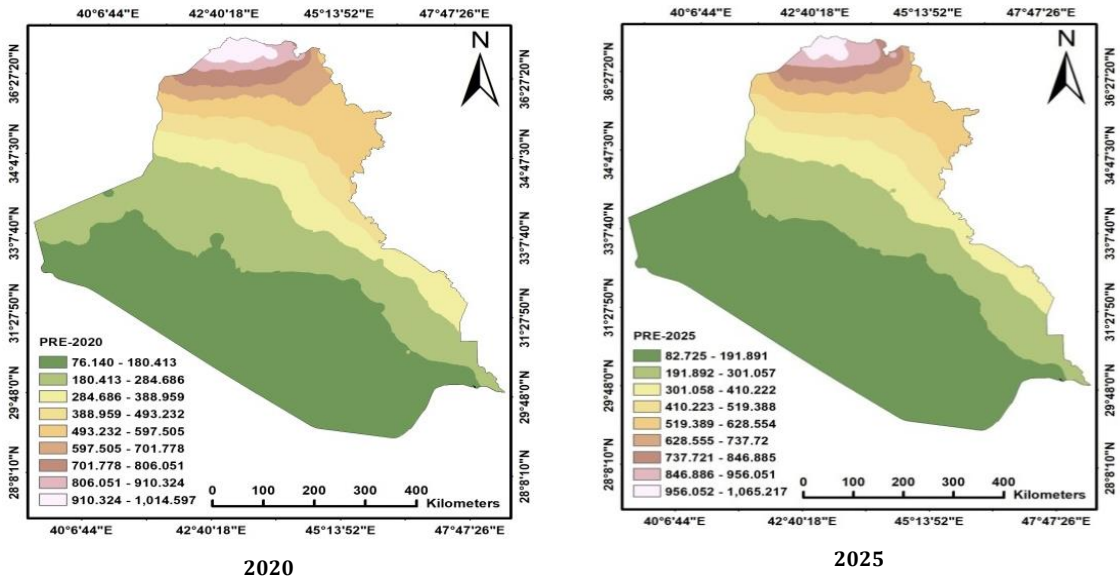

Figure 4: Distribution of precipitation extracted values over the period from 1956 to 2025

In conclusion, table 3 represents the precipitation for each five years, according to long-term precipitation analyses done for Iraq over the period of time from 1956 to 2025, the country has a climate with considerable variation and generally stable average temperature ranges throughout the study period; specifically, the annual average measurable rainfall total has ranged mostly from 534 mm to 602 mm throughout most of the studied 70-yr time period. The maximum amount of measurable rain occurred during the 5-yr period from 1986-1990, when the average amount was 601.99 mm, and the maximum total during this period was 1,091.001 mm. The period from 1956-1960 was also when the country recorded its lowest level of measurable rain (only 21.622 mm) during this 70-year period. More recent averages (2011-2020) are slightly below those recorded during this period after experiencing their highest levels of measurable rain during the 20-year periods prior; however, the projected average for 2021-2025 should be near the average of 573.97 mm for this time period.

Table 3: Precipitation values summary in Iraq per five years for the period (1956-2025)

Period	Min. Precipitation (mm)	Max. Precipitation (mm)	Avg. Precipitation (mm)
1956 – 1960	21.622	1047.257	534.44
1961 – 1965	32.160	1080.289	556.22
1966 – 1970	105.204	1082.941	594.07
1971 – 1975	111.644	1037.845	574.74
1976 – 1980	110.338	1021.473	565.91
1981 – 1985	98.544	1010.672	554.61
1986 – 1990	112.980	1091.001	601.99
1991 – 1995	112.100	1071.736	591.92
1996 – 2000	65.110	1029.503	547.31
2001 – 2005	114.254	986.222	550.24
2006 – 2010	117.984	960.098	539.04
2011 – 2015	89.232	987.072	538.15
2016 – 2020	76.140	1014.597	545.37
2021 – 2025	82.725	1065.217	573.97

4. Conclusions

The effects of climate change on ecosystems, human populations, and financial institutions are substantial. Changes to water supplies, ecosystems, and weather patterns can be sudden or gradual, depending on the impact. A study of Iraqi geography looked at the yearly precipitation concentration rates. Using yearly precipitation data from 1956 to 2025, this analysis utilized a high-resolution climate grid dataset. This study's main goal was to examine how climate change affected the decade, as well as the first and last five years of each. The use of GIS allowed the researchers to accomplish their goals for this study. Significant variation was seen in the rainfall data for Iraq from the sixth to the tenth decades of the second millennium. From 21 to 1,047 mm in the sixth decade, 32–1,080 mm in the seventh, 105–1,082 mm in the eighth, 110–1,037 mm in the ninth, and 98–1,091 mm in the tenth. The rainfall was usually tolerable throughout the first and second five-year intervals of each decade; however, there was a lot of variation. But in the first two decades of the third century, rainfall was much less intense. Between 89 and 987

millimetres of precipitation and 114 to 986 millimeters of precipitation, respectively, levels fell over this time. While the south and southwest received far less precipitation, the northeastern and northern parts of the nation had the heaviest downpours. As a result of major climatic alterations, average yearly rainfall has decreased over the last several decades, which is different from trends observed in the late 1900s. The precipitation totals ranged from 76 mm to 1,014 mm, with a little increase to 1,065 mm during the 2010s. Precipitation was regularly heavier in the hilly north than in the dry south. The problem is going to become worse for Iraq, which is already dealing with the fallout of less rain and unpredictable weather. Therefore, it's critical to find other ways to get water and make the most of what rain does fall.

REFERENCES

Al-Ansari, N., 1981. Suspended and solute loads on the Lower Diyala River, NA Al-Ansari, GT AL-Sinawi and AK Jamil. IAHS Publication (159), Pp. 225.

Al-Ansari, N., 2013. Management of water resources in Iraq: perspectives and prognoses. Engineering, 5(6), Pp. 667-684.

Al-Ansari, N., 2021. Topography and climate of Iraq. Journal of Earth Sciences and Geotechnical Engineering, 11(2), Pp. 1-13.

Al-Ansari, N., and Knutsson, S., 2011. Toward prudent management of water resources in Iraq. Journal of Advanced Science and Engineering Research, 2011(1), Pp. 53-67.

Al-Ansari, N., Asaad, N., Walling, D., and Hussan, S., 1988. The suspended sediment discharge of the river Euphrates at Haditha, Iraq: an assessment of the potential for establishing sediment rating curves. Geografiska Annaler: Series A, Physical Geography, 70(3), Pp. 203-213.

Al-Azawi, F., Hamid, H., Mohammed, H., and Muhammad, J., 2024. An assessment of the rainfall changes scenarios projection until 2050. A case study of Iraq. Sarhad J Agric., 40(3), Pp. 774-784.

Aljuhaishi, S., Al-Timimi, Y., and Wahab, B., 2025. Spatio-temporal Variation of Weather Systems and their Seasonal Variability in Iraq.

Awadh, S. M., and Al-Dabbas, M., 2024. The Geography of Iraq. Springer Nature.

Azpurua, M. A., and Dos Ramos, K., 2010. A comparison of spatial interpolation methods for estimation of average electromagnetic field magnitude. Progress In Electromagnetics Research M, 14, Pp. 135-145.

Beck, H. E., Van Dijk, A. I., Levizzani, V., Schellekens, J., Miralles, D. G., Martens, B., and De Roo, A., 2017. MSWEP: 3-hourly 0.25 global gridded precipitation (1979–2015) by merging gauge, satellite, and reanalysis data. Hydrology and Earth System Sciences, 21(1), Pp. 589-615.

Beck, H. E., Vergopolan, N., Pan, M., Levizzani, V., Van Dijk, A. I., Weedon, G. P., Brocca, L., Pappenberger, F., Huffman, G. J., and Wood, E. F., 2017. Global-scale evaluation of 22 precipitation datasets using gauge observations and hydrological modeling. Hydrology and Earth System Sciences, 21(12), 6201-6217.

Behrangi A., Khakbaz B., AghaKouchak A. 2021. A satellite precipitation fusion framework (SPFusion) to produce high-resolution rain fall products. Advances in Water Resources, 148: 103869.

Burrough, P. A., McDonnell, R. A., and Lloyd, C. D., 2015. Principles of geographical information systems. Oxford university press.

Cai, W., Borlace, S., Lengaigne, M., Van Rensch, P., Collins, M., Vecchi, G., Timmermann, A., Santoso, A., McPhaden, M. J., and Wu, L., 2014. Increasing frequency of extreme El Niño events due to greenhouse warming. Nature climate change, 4(2), Pp. 111-116.

Camera, C., Bruggeman, A., Hadjinicolaou, P., Michaelides, S., and Lange, M. A., 2017. Evaluation of a spatial rainfall generator for generating high resolution precipitation projections over orographically complex terrain. Stochastic Environmental Research and Risk Assessment, 31(3), Pp. 757-773.

Chen, F., Liu, Y., Liu, Q., and Li, X., 2014. Spatial downscaling of TRMM 3B43 precipitation considering spatial heterogeneity. International Journal of Remote Sensing, 35(9), Pp. 3074-3093.

Donat, M., Alexander, L.V., Yang, H., Durre, I., Vose, R., Dunn, R.J., Willett, K.M., Aguilar, E., Brunet, M., and Caesar, J., 2013. Updated analyses of temperature and precipitation extreme indices since the beginning of the twentieth century: The HadEX2 dataset. Journal of Geophysical Research: Atmospheres, 118(5), Pp. 2098-2118.

Esri ArcGIS Desktop Documentation. 2023.https:// desktop.arcgis.com/en/.

Fick, S.E., and Hijmans, R.J., 2017. WorldClim 2: new 1-km spatial resolution climate surfaces for global land areas. International journal of climatology, 37(12), Pp.4302-4315.

Ge, F., Zhu, S., Luo, H., Zhi, X., and Wang, H., 2021. Future changes in precipitation extremes over Southeast Asia: insights from CMIP6 multi-model ensemble. Environmental Research Letters, 16(2), Pp. 024013.

Goddard, L.M., Mason, S.J., Zebiak, S.E., Ropelewski, C.F., Basher, R., and Cane, M.A., 2001. Current approaches to season-to-interannual climate prediction.

Groisman, Pg.Y., Knight, R.W., Easterling, D.R., Karl, T.R., Hegerl, G.C., and Razuvaev, V.N., 2005. Trends in intense precipitation in the climate record. Journal of Climate, 18(9), Pp. 1326-1350.

Harris, I., Osborn, T.J., Jones, P., and Lister, D., 2020. Version 4 of the CRU TS monthly high-resolution gridded multivariate climate dataset. Scientific data, 7(1), 109.

Haylock, M., Hofstra, N., Klein Tank, A., Klok, E., Jones, P., and New, M., 2008. A European daily high-resolution gridded data set of surface temperature and precipitation for 1950–2006.Journal of Geophysical Research: Atmospheres, 113(D20).

Herold, N., Alexander, L., Donat, M., Contractor, S., and Becker, A., 2016. How much does it rain over land? Geophysical Research Letters, 43(1), Pp. 341-348.

Hu ZY, Zhou QM, Chen X, et al.2018.Evaluation of three global gridded precipitation data sets in central Asia based on rain gauge obser vations. International Journal of Climatology, 38(9): Pp. 3475–3493.DOI：10.1002/joc.5510.

Huffman GJ, Bolvin DT, Braithwaite D, et al., 2017.Algorithm Theoretical Basis Document (ATBD) Version 4.6 for the NASA Global Precipitation Measurement (GPM) Integrated Multi-satellitE Retrievals for GPM (I-MERG.

IPCC. 2021.Sixth Assessment Report.https://www.ipcc.ch/assessment-report/ar6/.

IPCC. 2014.Fifth Assessment Report.https://www.ipcc.ch/assessment-report/ar5/.

Jensen JR.2016.Remote Sensing of the Environ ment: An Earth Resource Perspective.Pearson.

Kareem, H.H., and Nassrullah, S.A., 2025. Impact of climate changes on Arizona State precipitation patterns using high-resolution climatic gridded datasets.Journal of Groundwater Science and Engineering, 13, Pp. 34-46.

Kareem, H.H., Alturfi, U.A., and Bashboosh, N.N., 2024a. Flood hazard mapping of USK river located in Wales, United Kingdom through performing the hydrological analysis of the digital elevation model and Landsat 8-OLI using GIS and remote sensing techniques. Water Conservation and Management, 8 (1), pp.87 – 96.

Kareem, H.H., Attaee, M.H., and Omran, Z.A., 2024b. Estimation the WATER RATIO INDEX (WRI) and AUTOMATED WATER EXTRACTION INDEX (AWEI) of bath in the United Kingdom using remote sensing technology of the multispectral data of Landsat 8-OLI.Water Conservation and Management, 8 (2), pp.125 – 132.

Liebmann, B., and Allured, D., 2005. Daily precipitation grids for South America. Bulletin of the American Meteorological Society, 86(11), pp. 1567-1570.

Liu XM, Yang TT, Hsu K, et al.2017.Evaluating the streamflow simulation capability of PERSIANN-CDR daily rainfall products in two river basins on the Tibetan Plateau. Hydrology and Earth System Sciences, 21(1): pp. 169–181.DOI：10.5194/hess-21-169-2017.

Maurer, E.P., and Hidalgo, H.G., 2008. Utility of daily vs. monthly large-scale climate data: an intercomparison of two statistical downscaling methods. Hydrology and Earth System Sciences, 12(2), pp. 551-563.

Mishra V, Thapa S, Jha M.2022.Spatio-temporal trends of precipitation over India using satellite based high-resolution gridded datasets.

Remote Sensing of Environment, 270:112605.DOI：10.1007/s13143-019-00120-1.

Morice, C.P., Kennedy, J.J., Rayner, N.A., Winn, J.P., Hogan, E., Killick, R.E., Dunn, R.J., Osborn, T.J., Jones, P.D., and Simpson, I.R., 2021. An updated assessment of near-surface temperature change from 1850: The HadCRUT5 data set. Journal of Geophysical Research: Atmospheres, 126(3), e2019JD032361.

Muter, S.A., Al-Jiboori, M.H., and Al-Timimi, Y.K., 2025. Assessment of spatial and temporal monthly rainfall trend over Iraq. Baghdad Science Journal, 22(3), pp. 910-922.

Najah, S., and Kadhum, J.H., 2025. Verification of the amount of annual rainfall using satellite images and GIS analysis in Iraq. Mustansiriyah Journal of Pure and Applied Sciences, 3(3), pp. 38-47.

Nastos, P., Kapsomenakis, J., and Philandras, K., 2016. Evaluation of the TRMM 3B43 gridded precipitation estimates over Greece. Atmospheric Research, 169, pp. 497-514.

Osborn TJ, Jones PD.2014.The CRUTEM4 land surface air temperature data set: Construction, previous versions and dissemination via google earth.Earth System Science Data, 6(1): pp. 61–68.DOI：10.5194/essd-6-61-2014.

Osborn, T.J., Jones, P.D., Lister, D.H., Morice, C.P., Simpson, I.R., Winn, J., Hogan, E., and Harris, I.C., 2021. Land surface air temperature variations across the globe updated to 2019: The CRUTEM5 data set. Journal of Geophysical Research: Atmospheres, 126(2), e2019JD032352.

Osborn, T., and Hulme, M., 1997. Development of a relationship between station and grid-box rainday frequencies for climate model evaluation. Journal of Climate, 10(8), pp. 1885-1908.

Seneviratne, S., Nicholls, N., Easterling, D., Goodess, C., Kanae, S., Kossin, J., Luo, Y., Marengo, J., McInnes, K., and Rahimi, M., 2012. Changes in climate extremes and their impacts on the natural physical environment.

Setianto, A., and Triandini, T., 2013. Comparison of kriging and inverse distance weighted (IDW) interpolation methods in lineament extraction and analysis. Journal of Applied Geology, 5(1).

Shekhar MS, Karmakar S, Ghosh S.2020.Future changes in precipitation extremes over South Asia using a multimodel ensemble of CMIP5 and CMIP6 simulations. Journal of Climate,33(10): pp. 4033–4053.DOI：10.1088/17489326/abd7ad.

Shi, H., Li, T., and Wei, J., 2017. Evaluation of the gridded CRU TS precipitation dataset with the point raingauge records over the Three-River Headwaters Region. Journal of Hydrology, 548, 322-332.

Song, X., Mo, Y., Xuan, Y., Wang, Q.J., Wu, W., Zhang, J., and Zou, X., 2021. Impacts of urbanization on precipitation patterns in the greater Beijing–Tianjin–Hebei metropolitan region in northern China. Environmental Research Letters, 16(1), 014042.

Sun, Q., Miao, C., Duan, Q., Ashouri, H., Sorooshian, S., and Hsu, K.L., 2018. A review of global precipitation data sets: Data sources, estimation, and intercomparisons. Reviews of geophysics, 56(1), pp. 79-107.

Swain S, Mishra SK, Pandey A, et al.2022.Spatiotemporal assessment of precipitation variability, seasonality, and extreme characteristics over a Himalayan catchment. Theoretical and Applied Climatology, 147(1): pp. 817–833.DOI：10.1007/s00704-021-03861-0.

Timmermans B, Wehner M, Cooley D, et al.2019.An evaluation of the consistency of extremes in gridded precipitation data sets. Climate Dynamics, 52(11): pp. 6651–6670.DOI：10.1007/s00382-018-4537-0.

Trenberth, K.E., 1997. Short-term climate variations: Recent accomplishments and issues for future progress. Bulletin of the American Meteorological Society, 78(6), pp. 1081-1096.

Trenberth, K.E., Dai, A., Rasmussen, R.M., and Parsons, D.B., 2003. The changing character of precipitation. Bulletin of the American Meteorological Society, 84(9), pp. 1205-1218.

Weng, Q., 2010. Remote sensing and GIS integration.

Yatagai, A., Arakawa, O., Kamiguchi, K., Kawamoto, H., Nodzu, M.I., and Hamada, A., 2009. A 44-year daily gridded precipitation dataset for Asia based on a dense network of rain gauges. Sola, 5, pp. 137-140.

Zambrano, F., Wardlow, B., Tadesse, T., Lillo-Saavedra, M., and Lagos, O., 2017. Evaluating satellite-derived long-term historical precipitation datasets for drought monitoring in Chile. Atmospheric Research, 186, pp. 26-42.

Zhang, L., Li, X., Zheng, D., Zhang, K., Ma, Q., Zhao, Y., and Ge, Y., 2021. Merging multiple satellite-based precipitation products and gauge observations using a novel double machine learning approach. Journal of Hydrology, 594, 125969.

Zhang, Y., and Cheng, J., 2019. Spatio-temporal analysis of urban heat island using multisource remote sensing data: A case study in Hangzhou, China. IEEE Journal of Selected Topics in Applied Earth Observations and Remote Sensing, 12(9), pp. 3317-3326.